NAVAL MEDICAL RESEARCH INSTITUTE

Bethesda, Maryland 20889-5055 NMRI 92-73 September 1992

(2)

STATISTICALLY BASED DECOMPRESSION TABLES VIII: LINEAR-EXPONENTIAL KINETICS

E. C Parker
S. S. Survanshi
P. K. Weathersby
E. D. Thalmann

Naval Medical Research
and Development Command
Bethesda, Maryland 20889-5044

Department of the Navy
Naval Medical Command
Washington, DC 20372-5210

NOTICES

The opinions and assertions contained herein are the private ones of the writer and are not to be construed as official or reflecting the views of the naval service at large.

When U. S. Government drawings, specifications, or other data are used for any purpose other than a definitely related Government procurement operation, the Government thereby incurs no responsibility nor any obligation whatsoever, and the fact that the Government may have formulated, furnished or in any way supplied the said drawings, specifications, or other data is not to be regarded by implication or otherwise, as in any manner licensing the holder or any other person or corporation, or conveying any rights or permission to manufacture, use, or sell any patented invention that may in any way be related thereto.

Please do not request copies of this report from the Naval Medical Research Institute. Additional copies may be purchased from:

National Technical Information Service
5285 Port Royal Road
Springfield, Virginia 22161

Federal Government agencies and their contractors registered with the Defense Technical Information Center should direct requests for copies of this report to:

Defense Technical Information Center
Cameron Station
Alexandria, Virginia 22304-6145

TECHNICAL REVIEW AND APPROVAL

NMRI 92-73

The experiments reported herein were conducted according to the principles set forth in the current edition of the "Guide for the Care and Use of Laboratory Animals," Institute of Laboratory Animal Resources, National Research Council.

This technical report has been reviewed by the NMRI scientific and public affairs staff and is approved for publication. It is releasable to the National Technical Information Service where it will be available to the general public, including foreign nations.

LARRY W. LAUGHLIN
CAPT, MC, USN
Commanding Officer
Naval Medical Research Institute

REPORT DOCUMENTATION PAGE

1a. REPORT SECURITY CLASSIFICATION: UNCL	1b. RESTRICTIVE MARKINGS
2a. SECURITY CLASSIFICATION AUTHORITY	3. DISTRIBUTION/AVAILABILITY OF REPORT: Approved for public release; distribution is unlimited
2b. DECLASSIFICATION/DOWNGRADING SCHEDULE	
4. PERFORMING ORGANIZATION REPORT NUMBER(S): NMRI 92-73	5. MONITORING ORGANIZATION REPORT NUMBER(S)
6a. NAME OF PERFORMING ORGANIZATION: Naval Medical Research Institute; 6b. OFFICE SYMBOL (If applicable)	7a. NAME OF MONITORING ORGANIZATION: Naval Medical Command
6c. ADDRESS (City, State, and ZIP Code): 8901 Wisconsin Avenue, Bethesda, MD 20814-5055	7b. ADDRESS (City, State, and ZIP Code): Department of the Navy, Washington, DC 20372-5120
8a. NAME OF FUNDING/SPONSORING ORGANIZATION: Naval Medical Research & Development Comman; 8b. OFFICE SYMBOL (If applicable)	9. PROCUREMENT INSTRUMENT IDENTIFICATION NUMBER
8c. ADDRESS (City, State, and ZIP Code): 8901 Wisconsin Avenue, Bethesda, MD 20814-5044	10. SOURCE OF FUNDING NUMBERS

PROGRAM ELEMENT NO.	PROJECT NO.	TASK NO.	WORK UNIT ACCESSION NO.
63713N	M0099	.01A	1002

11. TITLE (Include Security Classification)

(U) STATISTICALLY BASED DECOMPRESSION TABLES VIII: LINEAR-EXPONENTIAL KINETICS

12. PERSONAL AUTHOR(S)
PARKER, E.C., S.S. SURVANSHI, P.K. WEATHERSBY, AND E.D. THALMANN

13a. TYPE OF REPORT	13b. TIME COVERED	14. DATE OF REPORT (Year, Month, Day)	15. PAGE COUNT
Technical Report	FROM 08/90 TO 10/91	1992 September	60

16. SUPPLEMENTARY NOTATION

17. COSATI CODES			18. SUBJECT TERMS (Continue on reverse if necessary and identify by block number)
FIELD	GROUP	SUB-GROUP	Decompression sickness, maximum likelihood, probabilistic modelling, gas exchange kinetics

19. ABSTRACT (Continue on reverse if necessary and identify by block number)

Probabilistic models applied to diving decompression data have been successful in describing decompression sickness (DCS) occurrence and even time of DCS occurrence. This study explores a class of models using linear as well as exponential gas exchange kinetics to provide slower tissue washout than previous models. The models consist of 3 or 4 kinetic compartments, each of which can employ purely exponential (EE) or mixed linear-exponential (LE) kinetics. The risk of DCS is obtained from the single or double integration of the sum of compartment over-pressures. The resulting four models, EE1, EE2, LE1, and LE2 cover a broad range of gas kinetic possibilities. The data used in fitting these models are compiled from U.S. Navy, Canadian, and British chamber dive trials. There are 799 different dive profiles, representing 2383 man-dives, with a DCS incidence of 5.8% (131 DCS cases, 75 marginal cases). Time of DCS occurrence information is included for all

20. DISTRIBUTION/AVAILABILITY OF ABSTRACT	21. ABSTRACT SECURITY CLASSIFICATION
☒ UNCLASSIFIED/UNLIMITED ☐ SAME AS RPT. ☐ OTIC USERS	Unclassified

22a. NAME OF RESPONSIBLE INDIVIDUAL	22b. TELEPHONE (Include Area Code)	22c. OFFICE SYMBOL
Regina E. Hunt, Command Editor	(202) 295-0198	SD/RSD/NMRI

DCS and many marginal cases. Maximum Likelihood fitting of the four models to these data indicate LE1 to be the best fit. The LE1 Model is able to predict DCS occurrence in the fitted data, as categorized by type of dive profile, risk level, and time of DCS occurrence. LE1 is able to predict DCS occurrence well in most data not used for fitting, with the exception of profiles using high percentage O_2 breathing mixtures and some repetitive profiles.

TABLE OF CONTENTS

ACKNOWLEDGEMENTS

This work was supported by Naval Medical Research and Development Command Work Unit No. M0099.01A-1002. The opinions and assertions contained herein are the private ones of the authors and are not to be construed as official or reflecting the views of the naval service at large.

The authors are grateful to G.W. Albin for many of the early parameter estimation runs and to S. Cecire and J. Gaines for valuable editorial assistance.

INTRODUCTION

This report continues the analysis of probabilistic models applied to decompression diving. Previous probabilistic models have been shown to be successful in describing occurrence and even time of occurrence of DCS (1,5,7). While simple exponential tissue gas kinetics have been widely used in such modelling, the need for kinetics that would result in slower tissue washout has been noted (5,7). The emphasis of this report is a class of models that employ linear as well as exponential kinetics in an attempt to provide this slower washout.

These models are extensions of similar models developed and described elsewhere (1,4,7). Where previous models used single- or multi-exponential compartments to describe gas exchange kinetics, the present models use mixed linear and single-exponential kinetics in each of several compartments. The effect of adding linear kinetics is to lengthen the duration of risk accumulation for a given compartment time constant.

The data used in this report are taken from the available dive data described in detail in Report VII (6) of this series. A wide variety of dive profiles is included in this modelling effort, from submarine escape exposures with durations on the order of minutes to saturation dives on the order of days. Single, repetitive, and multi-level, as well as air and Mark-15 (0.7 ATA PO_2) dives, are represented. Time of symptom occurrence is included for all DCS and many marginal cases.

The models, having been fitted to the data, can be used to predict DCS outcomes in various data sets. Since time of symptom information is included in the data, these

models may be used to predict the time of DCS occurrence as well.

MODELS

Two types of tissue kinetics and two types of risk formulation lead to the four classes of models that are considered in this analysis. All are extensions of multi-tissue, single exponential decay models described in detail in previous publications (1,7). The current models differ in that they allow the use of linear (LE), as well as exponential (EE) kinetics, as described by Thalmann (4).

In previous models (1,7), tissue pressures have been described by purely exponential uptake and elimination. The models of this report similarly allow for exponential-only kinetics (EE) in response to a linear change in inspired nitrogen;

$$Ptiss(T) = A + B \cdot T + C \cdot e^{-\frac{T}{\alpha}}$$

where;

$$A = P_{I0} - \alpha \cdot R_I + (P_vO_2 + P_vCO_2 + P_IH_2O)$$

$$B = R_I$$

$$C = Ptiss_0 - (P_vO_2 + P_vCO_2 + P_IH_2O) - P_{I0} + \alpha \cdot R_I$$

Ptiss(T) is the compartment tissue pressure at the time of interest T, $Ptiss_0$ is the beginning tissue pressure, P_{I0} is the initial inert pressure, R_I is the rate of change of inert pressure over the time of interest, P_vO_2, P_vCO_2 and P_IH_2O are constant metabolic gas

pressures and α is the compartment time constant, sometimes expressed as a rate constant k, where $k = \alpha^{-1}$. For those more accustomed to half-times, the time constants reported here can be converted to half-times by multiplying α by 0.693.

The metabolic gas terms P_vO_2, P_vCO_2 and P_IH_2O were not included in earlier models (1,5,7), but are included here to acknowledge that non-inert gasses can contribute to gas bubbles (4).

In addition, the current models allow for mixed linear and exponential kinetics (LE). Linear kinetics are invoked whenever the tissue pressure exceeds ambient pressure by a given amount. This overpressure is represented in the model by the parameter PXO, with one PXO per tissue. When the tissue pressure falls below ambient plus PXO for that compartment, tissue pressure follows exponential kinetics. Linear kinetics are never invoked during gas uptake because tissue pressure never exceeds ambient while in uptake. This results in the desired asymmetry in gas uptake and washout, with washout occurring at a slower rate than uptake.

The shape of the linear kinetic curve is dominated by its slope, which is a function of the PXO and time constant for each compartment;

$$Ptiss(T) = Ptiss_0 + \frac{P_vO_2 + P_vCO_2 - P_ICO_2 - PO_0 - PXO}{\alpha} \cdot T - \frac{RO_2}{2 \cdot \alpha} \cdot T^2$$

where Ptiss(T) is the tissue pressure at the time of interest, $Ptiss_0$ is the initial tissue pressure, PO_0 is the initial oxygen pressure, P_vO_2, P_vCO_2 and P_ICO_2 are constant metabolic gas pressures, α is the compartment time constant and RO_2 is the rate of

change of oxygen pressure over the time of interest. The quadratic term will be non-zero only over periods with changing oxygen pressure, that is, $RO_2 \neq 0$.

So, for any given compartment time constant, the slope of the linear tissue pressure curve will be steeper for large values of PXO and shallower for small values of PXO. Thus, the lower the PXO value, the slower the washout for that compartment. Conversely, if the PXO is high enough, linear kinetics is not invoked and the LE model simplifies to the EE model.

In Fig. 1, the first frame shows the effect of adding a PXO parameter to a given tissue pressure curve for a single air dive. Both curves have the same time constant and gain. The curve with a PXO of 1000 fsw, and therefore no linear kinetics, decays exponentially. The curve with a PXO of 15 fsw invokes linear kinetics during ascent and remains in linear kinetics mode until Ptiss decays to 15 fsw. After surfacing, since oxygen pressure is not changing, the quadratic term will be zero and the kinetics will be linear. The kinetics remain in linear mode for this curve until about 280 minutes, when the tissue pressure drops below 15 fsw and the curve then decays exponentially, at the same time constant as in the exponential-only case. The mixed-kinetic curve crosses 0 fsw ambient pressure about 100 minutes later than the exponential-only curve. A tissue with a small PXO of around 1 or 2 would reach 0 fsw much later still.

Risk accumulation for each of these models is characterized by an instantaneous risk proportional to the sum of the risks of each compartment. In the first class of models the relative supersaturation in each of up to four tissues is used to define the instantaneous risk;

$$r1 = r1A + r1B + r1C + r1D$$

Where

$$r1A = GA1 \frac{PtisA - Pamb - ThrA}{Pamb} \qquad ; r1A \geq 0$$

with r1B, r1C and r1D defined similarly for each compartment. GA1 is a scale factor, PtisA is the tissue pressure for compartment A, Pamb is the ambient pressure and ThrA is the threshold parameter (1) for compartment A. Tissue pressure must exceed ambient plus the threshold in order for that compartment to generate a non-zero instantaneous risk. Models using this type of risk accumulation will be referred to as EE1 models when exponential-only kinetics is allowed, and as LE1 when linear-exponential kinetics is used.

Appendix A gives the details of the analytic risk calculation for the LE1 and EE1 class of models.

In the second class of models the risk is obtained from the integral of the relative supersaturation in each of up to three tissues;

$$r2 = r2A + r2B + r2C$$

Where;

$$r2A = GA2 \int_0^t \frac{PtisA - Pamb - ThrA}{Pamb} \, ds \qquad ; r2A \geq 0$$

with r2B and r2C defined similarly for each tissue and GA2, PtisA, Pamb, and ThrA defined as for the first model above. Models using this type of risk accumulation will be referred to as EE2 and LE2 models as defined for EE1 and LE1 models above.

In the first instantaneous risk plot of Fig. 1, the effect of the PXO parameter in delaying risk is shown in terms of the risk accumulated by the EE1 and LE1 algorithms. Since the thresholds for this example are set to 0, the instantaneous risk curves are proportional to the tissue pressure curves of the top plot. Again, the important difference is that the curve with a 15 fsw PXO accumulates risk about 100 minutes longer than the exponential-only curve.

This difference is greatly amplified in the second instantaneous risk plot of Fig. 1 due to the integration of the pressure difference used in EE2 and LE2 models. Parameter estimation inevitably reduces the gain of these models, EE2 and LE2 so that they have roughly similar total risks after long integration. Here, even the exponential-only (EE2) risk curve extends long after the end of the dive, coming back to 0 at about 1280 minutes. The mixed linear-exponential risk curve (LE2) is substantially lengthened, not decaying to 0 until almost 48 hours after surfacing. Smaller PXOs provide even more time at risk. It would seem that EE2 models have already achieved the desired extension of risk accumulation without the addition of linear kinetics.

However, simply lengthening the risk curve is not necessarily sufficient to provide a superior model. The shape of the risk curve, particularly how it relates to the time of symptom information in the data, is an important factor.

The parameters for each model, at minimum a time constant and gain for each compartment, with the option of a PXO and a threshold, are estimated from the data. The probability of each outcome, needed for the estimation, comes from the following equations;

if DCS *is not* observed;

$$P(no\ DCS) = e^{-\int_0^{24hrs} r\,dt}$$

if DCS *is* observed in the interval T1 - T2:

$$P(DCS) = (e^{-\int_0^{T1} r\,dt}) \cdot (1.0 - e^{-\int_{T1}^{T2} r\,dt})$$

The calculation of P(DCS) combines the probability of not observing DCS over the interval from 0 to T1 with the probability of observing DCS over the interval T1 to T2. Any risk remaining after T2 in this case is ignored, where in the case of no DCS, all risk out to 24 hours is included.

The Likelihood function is calculated as the product of all individual dive probabilities, P(outcome n);

$$L = P(outcome\ 1) \times P(outcome\ 2) \times \ldots P(outcome\ n)$$

Since each P has a value of less than 1.0, we use the natural logarithm of L, or the Log-Likelihood (LL).A modified Marquardt (3) nonlinear estimation algorithm is used to adjust the parameter values to be estimated in order to maximize LL. In general, many values of starting parameters must be tested with this estimation procedure in order to be certain that the maximum LL found is a global and not a local maximum. The shape of the likelihood surface near the converged parameters is used to estimate the precision of the parameters (2).

A simplified model, the Null model, assumes a constant instantaneous risk for all dives;

$r = 0$ *before beginning decompression*

$r = constant$ *after beginning decompression*

The LL value for the Null model can be considered as a baseline that more complex models must exceed.

DATA

The data sets used in fitting models in this report were taken from the dive data described in detail in Report VII (6) of this series. The 14 different data sets (Table 1) contain 799 dive profiles, representing 2383 man-dives. From these dives there are 131 DCS and 75 marginal cases, giving an overall incidence of 5.8%. Marginal cases are taken to be equal to 0.1 DCS case.

Marginal symptoms, sometimes called "niggles", are transient aches or pains following a dive and seemingly associated with it but not of a severity or persistence to warrant treatment.

In previous modelling (1,5,7), we assigned marginal cases a numerical outcome of 0.5. This assignment is functionally an implementation of the assumption that two marginal cases are as important as a single DCS case. Discussions with senior medical officers indicate a much lower level of concern for marginal outcomes. Furthermore, not all reports included marginal symptoms, thus raising the chance that data including them would appear excessively dangerous for DCS.

One region of the data where assignment of marginal outcomes is important is in the region of shallow saturation dives. This data contains 19 exposures to 25.5 fsw air for 2 days followed by rapid decompression. No DCS cases were recorded, but 17 marginal cases were observed (13 of them excessive fatigue). If marginal cases are considered as 0.5 DCS, then raw incidence from this depth is 45%; if they are considered as 0.1 DCS, then the incidence is 9%. The latter figure seems more appropriate, especially since there were no DCS and no marginal cases in the 32 saturation exposures

to 20 fsw in the data. Therefore, we chose to assign marginal cases as 0.1 DCS outcome throughout the data.

Of the 2383 man-dives, 36.8% were from the Single Air category, 8.1% were from Repetitive Air, 32.4% were Single non-Air, 10.0% were Repetitive non-Air, and 12.7% were from Air Saturation. Only dives with immersed subjects were included. Table 1 gives the distribution of profiles, man-dives, and DCS cases for each data set and category. Dives not included in the present data set, but described in Report VII (6) were single and repetitive air dives with dry subjects, those from oxygen decompression and surface decompression categories as well as some multi-level non-air dives. These dives and their relationship to the models will be discussed later.

Time of DCS occurrence is included for all full DCS cases and for many of the marginal cases. The time of symptom occurrence is represented in the data as an interval (T1-T2) over which symptoms appeared. T1 is taken to be the last known time the diver was entirely free of symptoms and T2 is the time at which definite symptoms were reported. Details of the methods and rules of establishing the T1-T2 times for a dive are given in Report VII. A listing of all DCS and marginal cases in the fitted data set, with T1 and T2 times, is given in Appendix B.

With the exception of two single air dives, all T2 times that occurred before surfacing were from the saturation data sets, where DCS occurrence under pressure is not uncommon.

Figure 2 shows the distribution of T2 times relative to time of surfacing for dives in which DCS (or a marginal) occurred. While a large number of cases occurred within a

few hours of surfacing, the rate of occurrence did not drop off substantially until eight hours after surfacing. Over 10% of all cases occurred more than eight hours after the dive surfaced.

RESULTS OF FITTING

The results of fitting the four classes of models to the data are summarized in Table 2, which gives the Log Likelihood (LL) values found for each of the various levels of complexity of the EE1, LE1, EE2, and LE2 models. There are three or four compartment versions with and without PXO, as well as with and without thresholds. Two compartment models of all four classes were tried but found to be much poorer fits than those presented here. Table 3 gives the parameter values found for the most important versions of each model.

The simplest form of both EE1 and EE2 are significantly better fits to the data than the Null model, with LL improvements of about 180 and 113 for Models 1a and 2a, respectively. Both of these are exponential-only models (PXO parameters fixed at values high enough that linear kinetics is never invoked) and have thresholds set to 0.0.

EE1 and LE1

Each step of added complexity does not always result in a significant improvement of fit. Significance of fit is measured by the Likelihood Ratio test (2,1). In this test, twice the difference of the log likelihoods of two models is an χ^2 distributed variable, with degrees of freedom equal to the number of added parameters, if the added parameters do not significantly improve the fit.

For example, a threshold parameter is added to each compartment of Model 1a to make 1b, three added parameters, but the fit improves by only 1.2 LL units. For the additional three parameters there would have to be an improvement in LL of at least 3.9 units for the more complex fit to be significant, even at the 95% level. Thus, the addition of thresholds to the EE1 model is not justified statistically.

Similarly, the two added parameters required to get Model 1c, a four-compartment EE1 model without thresholds, is not justified, since the LL improvement over 1a is only 0.22. Also, adding thresholds to two compartments to get Model 1d is not justified by an LL improvement of only 1.88.

To get Model 1e from 1a, a PXO parameter is added to each compartment, enabling mixed linear-exponential kinetics. However, only the PXO on the second compartment is statistically justified by the Likelihood Ratio test, so only one parameter is added to Model 1a to make 1e.

The significance of the single PXO parameter in the LE1 model was arrived at by adding a PXO to each compartment individually, as well as to all compartments together and using the Likelihood Ratio test to judge the benefit of each addition. The LL values for models with a PXO on only the first, second or third compartment are -707.35, -700.11 and -708.50, respectively and for a PXO on all three compartments the LL is -698.47.

With an LL value of -708.77 for Model 1a, only two of these models with added PXOs have a significant fit relative to 1a; the second and the fourth proposed models with improvement of 8.66 and 10.30, respectively. While the fourth of these test models,

with PXOs on all compartments, is certainly significant relative to 1a, it is not significant relative to the simpler second test model, with a PXO on the second compartment only. Since the LL improvement between these two models is only 1.64, compared to the χ^2 value of 3.0, the more complex fourth model cannot be considered a significant improvement over the second test model. The fit of the second test model, with a single added parameter, is significant at the 99.5% level and is listed in Table 2 as Model 1e.

Addition of threshold parameters to Model 1e results in Model 1f. In this case adding only one threshold parameter, on the longest time constant compartment, is justified statistically following the method described above for adding PXO parameters. The LL improvement of 1f over 1e is 3.6 units, enough for significance at the 99% level.

Model 1f is the most complex three compartment LE1 model obtainable with a statistically significant fit to the data.

Model 1g is the four-compartment version of 1e, also requiring only one PXO parameter, on the second time constant compartment. Since 1g gives an improvement in LL of only 0.61, it is not significant relative to 1e.

Model 1h is the elaboration of 1f into four compartments, using eleven parameters. Like 1f, 1h has only one PXO parameter, but has two threshold parameters, one on each of the two longest time constant compartments. The addition of three parameters, time constant, gain and threshold, to make Model 1h requires an LL improvement of at least 8.1 units for significance at the 99.9% level. Since the actual improvement is 8.8 units, Model 1h is significant and is the most complex fit of the LE1 risk models. Note in Table 3 that the parameters for the first three compartments of Model 1h are virtually

identical to those of Model 1f. The only exception being the third compartment gain, which is about 13% smaller for 1h, giving this compartment relatively less importance in 1h than 1f while the kinetics remain unchanged.

The long time constant of the fourth compartment, along with its 30.6 fsw threshold, insure that this compartment will not contribute to risk accumulation except in long, deep dives with fairly rapid decompression. In fact this compartment accumulates risk on only eight saturation profiles in the fitted data, from the data set ASATNSM. These dives saturated men at 111 fsw on air then quickly decompressed to 55 or 60 fsw, followed by a slower staged decompression to the surface. These eight profiles resulted in 8 DCS cases out of 17 man-dives. Since the gain for the fourth compartment is over 1000 times larger than that for the third, this compartment will certainly dominate the total risk on those dives, and any others which are able to invoke it.

It is because this compartment is involved with so few dives that the uncertainties in its parameters are so large. Despite its limited involvement, this fourth compartment contributes enough to the overall fit of the model that its presence is justified statistically.

For all of the LE1 models (1e, 1f, 1g, and 1h), only one compartment has a PXO parameter low enough to invoke linear kinetics. This is shown in Table 3 as PXOB, which is nearly identical for both Model 1f and 1h. With a PXO of 1.06 fsw, linear kinetics will be invoked on practically every profile in the data set since the tissue pressure for this compartment will often exceed ambient pressure plus this PXO. This compartment will remain in linear mode until the tissue pressure decays to 1.06 fsw over

the ambient, greatly lengthening the time extent of this compartment's overpressure compared to exponential-only kinetics. Since this compartment has no threshold parameter, risk will be accumulated during all of this decay time.

EE2 and LE2

As is the case for EE1 and LE1, added complexity does not always yield a significantly better fit for EE2 and LE2 models (Table 2). In adding three threshold parameters to 2a to make 2b, an improvement of 31.1 in LL is achieved, more than enough for significance at the 99.9% level. However, the addition of finite PXO parameters on any or all compartments does not result in a significant improvement in LL relative to the simpler exponential-only models. Model 2c has a poorer LL fit than 2b, with the same number of parameters. While Model 2d is a significant improvement over 2c, it is not significant relative to the simpler 2b, with an LL improvement there of only 0.70 for 3 added parameters. The improvement in LL between 2d and 2c is comparable to that between 2b and 2a and is due primarily to the addition of the threshold parameters. No LE2 model is significant relative to the simpler EE2 models.

The most significant fit of the integrated risk models is Model 2b, which has exponential-only kinetics with three separate thresholds but no finite PXO parameters. The values of its nine parameters are listed in Table 3.

The present data set does not require that linear kinetics be invoked in models of Type 2. The prolonged accumulation of risk due to the integration appears to be sufficient without the added duration afforded by linear kinetics. In trial fits with fixed values of PXO's, LE2's time constant parameters are adjusted to smaller values by the

fitting routine when lower PXO values are set, in an attempt by the model to offset the lengthening effect of linear kinetics.

Development of a four-compartment version of EE2 or LE2 is considered unnecessary due to its abundant coverage of all possible symptom times in three-compartment form.

Both models were successful in fitting the data using symptom times. Previous models ('Model 1' in (7)) similar to the current EE1 were unable to accommodate certain symptom times in this data set. On several dives the instantaneous risk of each compartment in those models decays to zero before reaching the beginning of the T1-T2 interval for that dive, resulting in an impossible outcome; occurrence of DCS during a period of zero risk, and thus an infinite LL.

From the finite LL values in Table 2, it is clear that even the current EE1 models (1a, 1b, 1c, and 1d) were able to fit *all* of the symptom time data. The reason for this apparent contradiction lies in the treatment of metabolic gases O_2, CO_2, and H_2O which are ignored in the previous models (1,7) and are here given constant non-zero values. These metabolic gases have the effect of adding a constant offset of about 0.1 ATA to the total tissue pressure. The pressure that any tissue will reach in a given uptake time is now increased by that small amount. Off-gassing to an ambient pressure of 1 ATA requires more time for this tissue than for the previous model, having started its decay from a higher pressure. This added time is enough to allow an exponential decay curve to reach the symptom times previously missed.

To illustrate, in Fig. 3 tissue pressures are plotted for a single compartment of the current EE1 model and the previous model using the same compartment time constant. The ambient pressure is provided by one of the dives from the fitted data set that the previous model was unable to fit. The difference due to the metabolic gases is clear in the constant offset between these two otherwise identical curves. The T1 marked in the figure is the critical point at which the tissue pressure must exceed 1 ATA in order to 'fit' this dive. The previous model's tissue pressure, and thus its risk, decays below 1 ATA more than an hour before T1, while for the same time constant, EE1 sustains pressure almost 10 minutes beyond T1, giving EE1 a small but important instantaneous risk within the T1-T2 interval. While other time constants may allow the previous model's tissue pressure to come closer to T1 for this dive, no time constant is capable of reaching it (7).

Because this added decay time is not needed by EE2 or LE2 to satisfy these symptom times, they accommodate the metabolic gases in a different way. Previous models (Model 2 in (7)), similar to the current EE2, with exponential-only kinetics, but ignoring metabolic gases, were able to fit all of the symptom time data. With the metabolic gases present, as they are in Model 2b, each tissue requires a threshold parameter that ranges from 2.6 to 3.8 fsw. The offset of ≈0.1 ATA generated by these gases equates to a ≈3.3 fsw difference in tissue pressure, close to the average found for thresholds when these gases are present. The effect of these thresholds is to decrease the accumulation of risk by roughly the same amount it is increased by the metabolic gases. If the metabolic gases are set to zero in EE2, making this model the same as the

previously published model, no thresholds are supported.

The LL value for that previous model is -748.7 for the current data set, while for Model 2b it is -744.2, suggesting that there is some additional improvement in fit due to including the metabolic gases beyond the compensating effect of the thresholds. The remaining parameters are virtually identical in both cases, except for a 24% decrease in the middle compartment gain when the metabolic gases are present.

Model 2b, therefore, compensates for the addition of these gases by requiring offsetting thresholds for each compartment, negating the effect of the increase in total tissue pressure.

ESTIMATES FOR INDIVIDUAL DATA SETS - FITTED

These models, having been "calibrated" by fitting them to the current dive data set, can now be used to predict the probability of occurrence of DCS in any proposed or actual dive profile. By using the best fitting models to predict occurrence in subsets of the data to which they were fit, we have a further test of the values and limitations of each model. The results of these predictions are shown in Table 4.

Models 1f and 1h give nearly identical results in almost all cases. The only difference greater than 1 DCS case arises in the saturation data, as might be expected, since the fourth compartment that sets 1h apart from 1f is only invoked in these data, as noted in the fitting of Model 1h. While differences in predictions between 1f and 1h are in the 1 to 4% range elsewhere, in the saturation data the differences are approximately 7 to 12%.

Model 2b does a better job of predicting DCS in 8 out of 14 individual data sets than either 1f or 1h, but does slightly worse in the overall prediction. Looking at data groups, 2b does better in predicting DCS in Single Air and Repetitive Non-Air, but tends to over-predict, leading to a higher overall total compared to 1f and 1h.

From Table 4, Model 1f would appear to be the best predictor of DCS occurrence among the original data, but only by a slight amount. No model stands out from this test to be strongly preferred over the others. In fact, all three predict occurrence fairly well in these data.

Figure 4 is a graphical presentation of the information in Table 4, with the addition of error bars representing the 95% confidence limits of each prediction. The large uncertainty associated with Model 1h in saturation data is due to the large standard errors of the fourth compartment's parameters (Table 3). Since this compartment contributes to risk accumulation only in the few saturation dives noted above, the uncertainty in its parameter values does not influence predictions in other data. The large uncertainty for this model in the combined data is inherited from this effect in the saturation data.

From Fig. 4 it is clear that, except for the differences noted above, Models 1f and 1h are virtually identical. However both of these models fail to contain the observed value for Repetitive Non-Air within its error bars. Only Model 2b brackets the observed DCS values in every case.

Table 5 presents another test of each model's ability to predict occurrence among the fitted data. In this method, each model is used to classify all of the fitted dives into risk level groups as shown in the first column. From these groups, which may contain a different number of dives for each model, the number of DCS cases observed and the model's prediction of occurrence is reported. This provides a measure of how well a model can distinguish between dives of different risk. The risk limits were chosen to allow as even a distribution of dives among the risk categories as possible without resorting to awkward limited groups.

Again, Models 1f and 1h have similar results, with the exception that 1h predicts occurrence in the highest risk category slightly better than 1f. Their observed and predicted values are almost identical in the lowest risk group, with both under-predicting by about 30%.

Model 2b follows the same pattern of over and under-prediction as 1f and 1h, under-predicting somewhat more (40%) in the lowest risk group. The distribution of dives, and of DCS cases, is different for 2b with fewer dives and cases observed in the extreme groups and more in the middle range. Revising the risk limits to give Model 2b a more even dive distribution improves its DCS prediction for the lowest risk group, which then under-predicts by only 4%. This arrangement gives results similar to those of 1f and 1h in all other risk groups.

The χ^2 statistics listed in Table 5 for each model are a measure of the frequency with which random variation would be expected to lead to the observed lack of agreement. The Null model can be conclusively rejected ($p<0.001$) as disagreeing with

the data. Models 1f, 1h, and 2b cannot be rejected ($p>.05$). While Model 1h nominally has the lowest χ^2 value, the similarity of the values for 1f, 1h, and 2b does not allow this statistic to distinguish between these three models.

No strong preference for any model can be drawn from this test as all three models are able to separate the fitted dives by risk with about the same level of accuracy.

Another test of model performance, this one measuring a model's ability to predict time of symptom occurrence, is presented in Table 6. With the inclusion of symptom times in the fitted data, these models should be capable of distinguishing between dives by their time of symptoms. Time categories are constructed relative to surfacing time of the dive, and the number of observed DCS cases is calculated from the proportion of each T1-T2 interval falling in each category. Only single-dive records are included in this test due to the difficulty in choosing surfacing time for repetitive dives.

Table 6 shows that the Null model fails to predict the time of DCS occurrence. This constant risk model predicts DCS occurrence as an exponentially decaying function. However, the time constant of this decay is the reciprocal of the risk, and is therefore very long (≈33,000 min). Thus, for times of up to 24 hours, the Null model predicts DCS occurrence as virtually constant, proportional only to the length of the time interval. This results in far too much risk being placed long after surfacing when fewer actual DCS cases are observed.

Once again it is difficult to distinguish between Models 1f and 1h. They both predict time of occurrence much better than the Null model and they miss their predictions in the same direction and nearly the same proportion for each time category.

Model 2b is also a great improvement over the Null model and performs comparably with 1f and 1h, except for DCS times before surfacing where 2b does poorly. From the example given in Fig. 1 it is clear that Model 2b will continue to have risk accumulation beyond the 24-hour limit of Table 6 for some dives. However, this is true for fewer than 4% of all fitted dives, and half of these only extend risk to between 24 and 25 hours. The effect of including this later risk is a slight increase in predicted DCS in the last time category, making no change in any conclusions drawn from this test. Models 1f and 1h do not have risk accumulation beyond 24 hours after surfacing.

Based on the χ^2 values for this test, the Null model can be conclusively rejected ($p<0.001$), while Models 1f, 1h, and 2b are accepted as representing the data. However, because of the similarity in χ^2 values for these three models, again this statistic does not distinguish between them.

ESTIMATES FOR INDIVIDUAL DATA SETS - NON-FITTED

Applying these models to predict occurrence in dives not included in the fitted data reveals some of their limitations. Table 7 lists the results of these predictions with their 95% confidence limits.

The Single and the Repetitive air data listed in Table 7 are the "dry subject" counterparts to similar data with "wet subjects", which were used in model fitting. DCS occurrence in data set DC4D is predicted reasonably well by each of the three models, with an accuracy similar to that for Single Air dives in Table 4, suggesting that DC4D could reasonably be included in the fitted data. This is supported by the results of a

specific study of wet and dry single air dives (8), which concluded that the difference in risk is probably less than 30%.

Occurrence in DC4DR is badly over-predicted by all three models. A close look at DC4DR reveals that it contains two types of repetitive dives: No-decompression profiles unique to this data set and decompression profiles shared with DC4WR.

The no-decompression data consists of 93 man-dives in which no DCS cases were observed; the models predict about 3 cases due to an underlying average risk of about 3%. The remaining 6 profiles of DC4DR are identical to the 6 profiles of DC4WR. So, why are these dives over-predicted in DC4DR and under-predicted in DC4WR? These profiles are considered by the models to have risk levels of 8 to 9.5%, and although the number of divers for each profile is different for DC4DR and DC4WR, the predicted average underlying risk for each is nearly the same, about 8.4%. For these profiles in DC4DR, 1 DCS case out of 49 man-dives was observed and over 4 cases are predicted, while these same profiles in DC4WR had 3 cases observed out of 12 man-dives but only 1 predicted. The models correctly see these profiles as generating the same risk, but 49 divers at 8.4% risk predicts over 4 DCS cases, while 12 divers at the same risk predicts only 1 case.

DCS occurrence in the repetitive non-air data set, EDU1180R, is over-predicted by all three models by 400 to 600%. The data set most similar to EDU1180R is EDU184 in which occurrence is only moderately over-predicted (12 to 33%). There are three main differences between these data sets: 1) during the interval between dives, EDU1180R profiles stay at 30 or 10 fsw, while those of EDU184 stay at the surface; 2)

EDU1180R divers breathed 0.7 ATA PO_2 throughout the dives, while in EDU184 air was breathed during the surface interval and 0.7 ATA PO_2 at depth; and 3) 0.7 ATA PO_2 gas was breathed for about 5 minutes on the surface before diving in EDU1180R. However, these differences seem to make EDU1180R's predicted DCS lower than it would otherwise be: If EDU1180R's profiles are artificially changed so that they go to the surface between dives and breath air while on surface, making them as close as possible to EDU184's, predicted DCS for this modified EDU1180R increases to 16.5, 15.8, and 15.8 cases from models 1f, 1h and 2b, respectively.

The very nature of EDU1180R's dives leads to the lowest possible predictions by the models, yet its DCS occurrence is still badly over-predicted. With so little data of this type available it is difficult to draw a firm conclusion from these discrepancies. The only way to resolve them is to add more multi-level and repetitive non-air dives to the data base to find whether EDU1180R represents a separate class of dives or is simply a statistical outlier, a highly improbable but still possible outcome.

The Air and O_2 Decompression data are not included in the original fitted data because they contain periods of high percentage oxygen breathing, close to 100% O_2. The current models were not expected to perform as well with such a gas mixture. The models treat the sudden loss of inspired N_2 pressure as leading to a rapid decrease in instantaneous risk. These models tend to systematically under-estimate the risk of this type of dive, as shown in Table 7. Models that fit well to dives having a high percentage oxygen breathing gas might need to allow for a continued risk presence despite the lack of nitrogen pressure.

The Surface Decompression dives of Table 7 have much in common with the Air and O_2 Decompression dives discussed above. The majority of these profiles have periods of high percentage oxygen breathing, in addition to rapid ascents to surface with a quick return to depth to resume decompression. DC8ASUR in particular seems closely related to the previous category, as its DCS is under-predicted, on average, by the same amount as for the Air and O_2 dives (about 60%).

Occurrence in DCSUREP, which combines repetitive dives with intermittent oxygen as well as surface decompression, is predicted well by all three models. This quality of prediction may suggest that the repetitive aspect of these dives is the dominant factor in how the models view them, as DCS occurrence in Repetitive Air dives is similarly well predicted (Table 4). Approximately 25% of these man-dives are wet exposures, 75% dry.

SUREX contains long saturation dives with short excursions to the surface and short periods of high O_2 gas breathing. While models 1f and 2b under-predict DCS in this data set by 20 to 50%, 1h over-predicts it by 350%. These profiles invoke the longest time constant compartment of Model 1h more than any other available set of dives. Due to the large gain on this compartment's risk, it assigns a large amount of risk to each of these dives, considering them all to be nearly 100% risky. The 24 SUREX dives are predicted by Model 1h to lead to 23.9 DCS cases.

Predictions of occurrence for the non-air saturation data set ASATARE are good, fair, and poor for Models 1f, 1h, and 2b respectively. Dives in this data set saturated at depths ranging from 23 to 78 fsw breathing 0.4 ATA O_2, followed by various excursions

to shallower depths while breathing air. About 13% of these dives used intermittent 100% O_2 with air breaks during excursions. While these gas mixtures set this data apart from the other saturation data, predictions of DCS in ASATARE are remarkably similar to those for ASATEDU, with each model giving nearly the same proportion of under-prediction for both of these different sets of data. The fact that Model 1f is a good predictor of DCS in ASATARE suggests that this data could be included with the fitted data for this model.

One measure of the ability of any of these data sets to be included into the fitted data set is how accurately its observed DCS occurrence is predicted by the model. Since each model's prediction is based on the fitted data, if a model's predicted DCS agrees well with the observed value, then that data might reasonably be combined with the fitted data under that model.

We can establish as a rule that the observed DCS for a data set must be within a model's 95% confidence limits of prediction for that data set to be considered for inclusion in the fitted data. Following this rule, only DC4D, DCSUREP and ASATARE might be included under models 1f and 1h, although the extreme range of limits for ASATARE with model 1h would allow for any possible outcome and may be misleading. Likewise, only DC4D and DCSUREP might be included under model 2b.

DISCUSSION

Models 1f and 1h, as well as Model 2b, are able to fit the time of symptoms data, to predict the occurrence of DCS in a majority of the available data and to predict time

of symptoms in the fitted single dives. None of these models fails outright in these tests. They are not entirely equal in their success, however. Both Models 1f and 1h fit the data much better than 2b, by 48 to 56 LL units (Table 2). Since models 1f and 1h are not subsets of 2b, a strict likelihood ratio test is not possible to reject 2b on these grounds. However, the LL values strongly indicate that Models 1f and 1h better describe the data than does Model 2b. In addition, Model 2b does not predict overall occurrence in both fitted and non-fitted individual data sets as well as either 1f or 1h.

One possible explanation for this difference is in the shape of the instantaneous risk curve for each model (Fig. 1). Models 1f and 1h have risk curves, and therefore risk accumulations, which are relatively limited in time extent, even to the point of nearly missing some symptom times. Model 2b, however, even without linear kinetics, has risk curves which extend to great lengths of time, clearly to the detriment of fitting the data.

Adjustments of kinetic, gain and threshold parameters in models 1f and 1h can have a dramatic effect on the fit to the data, resulting in wide variation in LL and even missing a dive's T1-T2 interval altogether. Subtle changes in risk distribution, to match that of the data, are possible because of the sensitivity of the model to changes in parameters.

Similar adjustments in Model 2b have less effect because the risk curves have a duration that makes changes in their shape are less important. In the simple example of Fig. 1, the same change in PXO extends time at risk by 67% for LE1 over EE1 and by 120% for LE2 over EE2. For LE1 this increase meant that it could now generate risk at more possible symptom times. Since the EE2 curve already covered almost all possible

symptom times, even such a large change is of little or no value. Adjustment of other available parameters results in similarly diluted effects. Subtle and controlled changes in adding risk for one dive or reducing it for another are more difficult with EE2.

The only distinction between Models 1f and 1h is in whether the fourth compartment of 1h makes a positive or a negative contribution. In terms of LL improvement, Model 1h is a significantly better fit to the data than 1f. But what does that fourth compartment really add to the value of the model? In the several tests of ability to predict DCS that were conducted, Model 1h did not distinguish itself as the superior model. Overall, Model 1h performs somewhat less well, over and under-predicting in slightly higher proportions, than Model 1f. A more troubling difference is illustrated in Fig. 4 and in the Model 1h prediction for the data set SUREX in Table 7, where the effect of the poorly determined fourth compartment parameters is clearly apparent.

While Model 1f is not the best overall fit, by LL, to the data set, the increased uncertainties and added complexity of the better fitting four compartment model make 1f the best overall model for the present data. Almost nothing is given up in terms of predictive ability in selecting Model 1f over 1h, and what is gained in simplicity and reduced predictive errors, particularly on saturation data, makes up for the penalty in LL fit.

Of the previously published models, 'Model 1' in (7) is closest in form to the current EE1, but was unable to fit some time of symptoms data, as discussed above, so its predictions of DCS are based on an occurrence-only scheme. Within the current

fitted data, the average difference in prediction between that older model and the current best fit model (1f) is only 0.9 cases. Ten of the 14 fitted data sets are better predicted by the LE1 model (1f). For the data not fitted, the average difference in prediction is just 0.8 cases, with only 3 of the 9 data sets better predicted by the current model. However, since many of these data sets are poorly predicted by both models, indicating one or the other as predicting such a data set "better" has little meaning.

The generally small differences between predictions from these two models suggests that each does well for the limited purpose of predicting DCS occurrence only. However, without time of symptoms information, the earlier model fails to predict time of occurrence (7), which the current model does well (Table 6). This limits the usefulness of the older model to applications in which timing is unimportant.

The predictions of the previously published model closest in form to the current EE2 ('Model 2' in (7)) can be compared directly with Model 2b, since the only difference between them is the presence of metabolic gases, as described above. Amongst the fitted data the average difference in prediction is just 0.4 cases, with a maximum difference of 1.7, while for the non-fitted data it is 0.3 cases, with a maximum of 0.7. Clearly there is little difference between these two integrated risk models in terms of their ability to predict DCS occurrence in any of the data. In addition each does quite well in predicting time of occurrence (Table 7; (7)). The small LL improvement (4.5 units for 3 added threshold parameters) for the current EE2 over the older model also does not indicate any strong difference between these two nearly identical models.

The only systematic failure of the current best model is in predicting DCS occurrence in dives with high O_2 breathing gas mixtures, especially when breathed during decompression. DCS occurrence on such dives as a group is under-predicted by 60%. As a test, the high O_2 data can be added to the original fitted data and a model of type 1f fitted to this combination. The DCS predictions that result from this fitting are better for the O_2 data, with DC8AOW, DC8AOD, and DC8ASUR now having a predicted 0.7, 3.5, and 6.0 cases respectively, an average 77% increase in predicted DCS. While this increase is an improvement for these O_2 data, there is a simultaneous increase in most other data set DCS predictions as well. In order to achieve a better fit to the O_2 data, this model simply increases risk accumulation for all dives. The net effect of these increases is an overall prediction of 144.2 DCS cases for the original fitted data (138.5 observed) compared with 138.9 predicted by Model 1f when using only the original fitted data (Table 4).

From the parameter values for this O_2 augmented fit, the increased risk accumulation is due primarily to reducing the threshold parameter on the longest time constant compartment from 1.74 (Model 1f) to 0.43 fsw. Because this 1.3-fsw difference occurs near 0 fsw, where the slope of the exponential decay curve is generally fairly flat, even this small change in threshold adds a great deal to risk accumulation time.

Further model development should include treatment of high O_2 gases such that they are not considered overwhelmingly safe, while allowing for appropriate fitting to a: dives.

The model's failure to predict DCS well on other data sets is not as troubling since the failure is not applied to a whole class of dives but to two isolated sets of profiles. These problematic data sets, DC4DR and EDU1180R, both badly over-predicted, have counterparts in the fitted data that appear to differ from them subtly at most and which are themselves predicted reasonably well. Inclusion of more quality data of the type found in each of these problematic data sets may resolve the questions raised by their failures here.

The use of linear-exponential kinetics in these models is somewhat limited, but significant where it is invoked. In LE1, only one of three or four compartments was found to require the mixed kinetics, the other compartments fitting better, or equally well, with exponential-only washout. In LE2, none of the compartments required mixed kinetics for a statistically significant fit.

The inclusion of these mixed kinetics in LE1 allowed an improvement of 12 LL units in fit over exponential-only EE1 models. The LE1 model also had a better fit than EE2 models by 48 LL units, and 52 LL units better than the exponential-only "Model 2" of (7). A direct comparison with "Model 1" of (7) is not possible, since that model is unable to fit the current data using time of symptoms information.

REFERENCES

1. Hays, J.R., B.L. Hart, P.K. Weathersby, S.S. Survanshi, L.D. Homer, and E.T. Flynn. Statistically based decompression tables IV. Extension to air and N_2O_2saturation diving. NMRI Technical Report No. 86-51, Naval Medical Research Institute, Bethesda, Maryland, 1986b.
2. Kendall, M.G. and A. Stewart. The Advanced Theory of Statistics. 4th ed. Vol. 2. London: Haffner, 1979, p. 38-180.
3. Marquardt, D.W. An algorithm for least-squares estimation of non-linear parameters. J. Soc. Indust. Appl. Math. Vol. 11, pp. 431-441, 1963.
4. Thalmann, E.D. Phase II testing of decompression algorithms for use in the U.S. Navy underwater decompression computer. NEDU Technical Report, No. 1-84, Navy Experimental Diving Unit, Panama City, Fla., 1984.
5. Weathersby, P.K., S.S. Survanshi, L.D. Homer, B.L. Hart, R.Y. Nishi, E.T. Flynn, and M.E. Bradley. Statistically based decompression tables I. Analysis of standard air dives: 1950 - 1970. NMRI Technical Report No. 85-16, Naval Medical Research Institute, Bethesda, Maryland, 1985a.
6. Weathersby, P.K., S.S. Survanshi, R.Y. Nishi, and E.D. Thalmann. Statistically based decompression tables VII. Primary data for testing human N_2O_2 decompression models. NMRI Technical Report No. 92-?, Naval Medical Research Institute, Bethesda, Maryland, 1992.

7. Weathersby, P.K., S.S Survanshi, L.D. Homer, E.C. Parker, and E.D. Thalmann. Predicting the time of occurrence of decompression sickness. Journal of Applied Physiology, Vol. , pp. 1992.

8. Weathersby, P.K., S.S. Survanshi, and R.Y. Nishi. Relative decompression risk of dry and wet chamber air dives. Undersea Biomedical Research, Vol. 17, No. 4, 1990.

APPENDIX A

LE1/EE1 Risk Calculation

The contribution to accumulated risk of any one time segment in the data is calculated analytically. This is achieved through a series of decisions based on the value and derivative of the instantaneous risk function during the time segment. Figure A1 shows the logical branching of these decisions for LE1 and EE1 type models. A similar, but far more complex figure could be prepared for LE2/EE2 model risk calculations. However, since neither LE2 or EE2 were selected as best-fitting models in this analysis, only the process for LE1/EE1 is included here.

The following terms are used in Fig. A1;

B1, B2, B12, ...B22211 are labels for the logical branches showing the path followed.

f(t) is the value of the instantaneous risk function at time t;

$$f(t) = \frac{Ptiss(t) - Pamb(t) - Thr}{\overline{Pamb}}$$

where, Ptiss(t) is the time varying tissue pressure which follows either quadratic/linear or exponential kinetics; Pamb(t) is ambient pressure, a linear function of time; Thr is the risk threshold, a constant; and Pamb in the denominator is the mean ambient pressure over this time segment.

f'(t) is the derivative of the instantaneous risk function at time t.

T_0 is the time at the beginning of the current segment.

T_E is the time at the end of the current segment.

T_X is the time at which $f'(t) = 0.0$

T_R is the time at which $f(t) = 0.0$, or the root of $f(t)$. There may be two roots in one time segment; T_{R1} and T_{R2}.

ΔR is the risk contribution due to the current time segment.

To illustrate the method by which a risk contribution is determined using this process, we can look at two quite different branches, B111 and B22211.

B111. Beginning with the value of the instantaneous risk function at time T_0, $f(T_0)$, this process can follow either the upper set of branches if the value is greater than 0, or the lower set if it is less than or equal to 0. In this case it follows B1, because $f(T_0)$ is positive. Next $f(T_E)$ is evaluated and for this case found to be also positive, leading to B11. At this point the first derivative of the risk function at time T_0 is used to choose the next branch. If $f'(T_0)$ is negative, several possibilities arise leading to three possible values of ΔR. However, in this case $f'(T_0)$ is positive (or 0.) and the value of ΔR for this segment is the integral of f(t) over the T_0 T_E interval.

B22211. For this path, the value of f(t) was found to be negative (or 0.) at T_0 and T_E, leading to B2 and B22. Then the derivative of $f(T_0)$ was found to be positive, leading to B222. At this point, if the derivative of f(t) at T_E is positive, then the function must take only negative values over this time segment. This leads to path B2222 and a risk contribution of 0 for this segment. However, in this example, $f'(T_E)$ is negative, meaning that there is a possibility of f(t) taking a positive value between T_0 and T_E. The

solution is to evaluate f(t) at the inflection point, the point at which $f'(t) = 0$. If f(t) at his point, T_X, is negative, then the function must take only negative values over this time segment, again leading to a risk contribution of 0.0 for path B22212. If $f(T_X)$ is positive, the function must have two roots, T_{R1} and T_{R2}, between which the function is positive. The risk contribution for this path, B22211, is the integral of f(t) over the interval between these two roots.

FIGURE A1

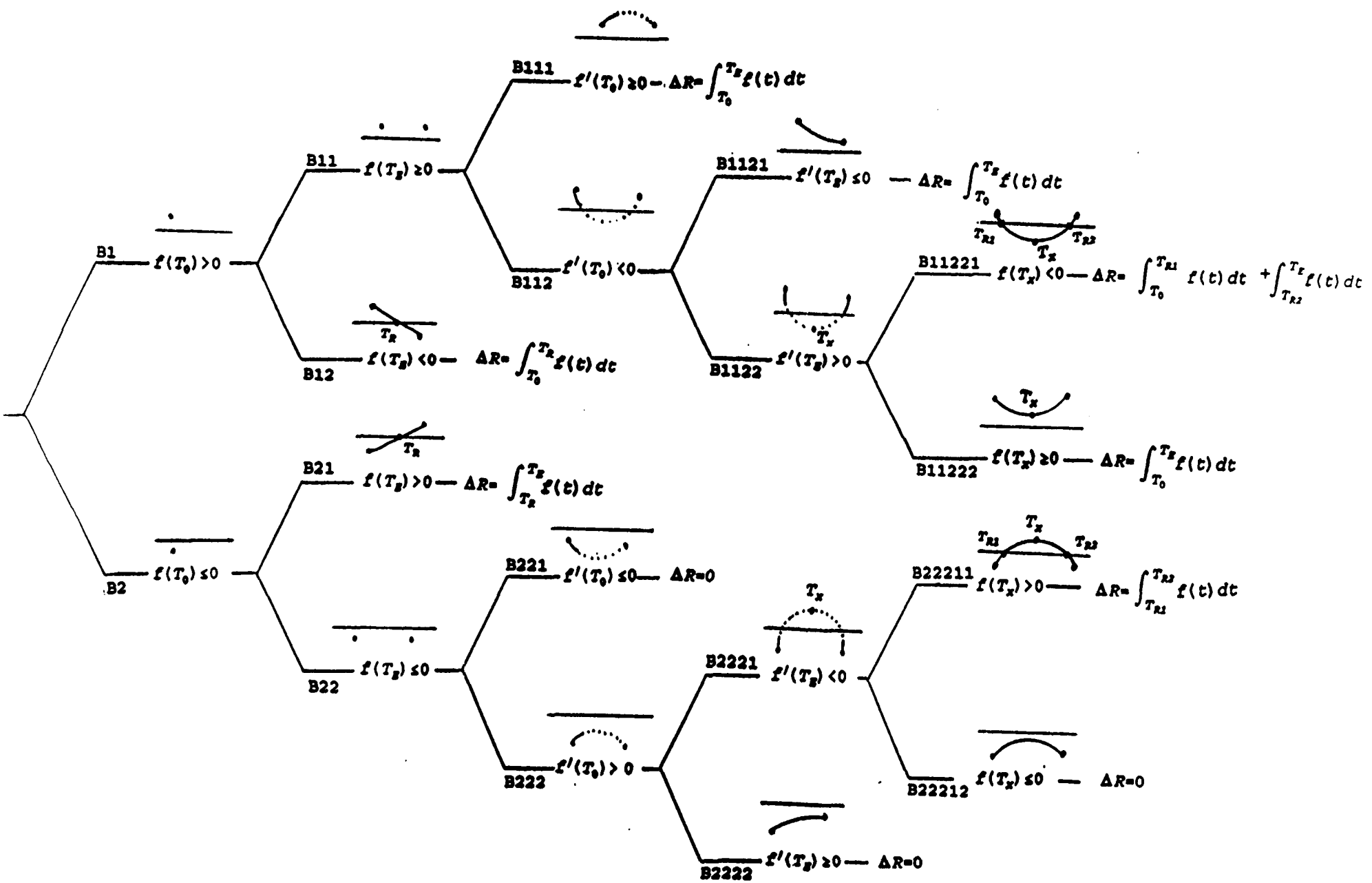
B1
$f(T_0)>0$
B11
$f(T_E)\geq 0$
B111
$f'(T_0)\geq 0$ — $\Delta R=\int_{T_0}^{T_E} f(t)\,dt$
B112
$f'(T_0)<0$
B1121
$f'(T_E)\leq 0$ — $\Delta R=\int_{T_0}^{T_E} f(t)\,dt$
B1122
$f'(T_E)>0$
B11221
$f(T_X)<0$ — $\Delta R=\int_{T_0}^{T_{R1}} f(t)\,dt+\int_{T_{R2}}^{T_E} f(t)\,dt$
B11222
$f(T_X)\geq 0$ — $\Delta R=\int_{T_0}^{T_E} f(t)\,dt$
B12
$f(T_E)<0$ — $\Delta R=\int_{T_0}^{T_R} f(t)\,dt$
B2
$f(T_0)\leq 0$
B21
$f(T_E)>0$ — $\Delta R=\int_{T_R}^{T_E} f(t)\,dt$
B22
$f(T_E)\leq 0$
B221
$f'(T_0)\leq 0$ — $\Delta R=0$
B222
$f'(T_0)>0$
B2221
$f'(T_E)<0$
B22211
$f(T_X)>0$ — $\Delta R=\int_{T_{R1}}^{T_{R2}} f(t)\,dt$
B22212
$f(T_X)\leq 0$ — $\Delta R=0$
B2222
$f'(T_E)\geq 0$ — $\Delta R=0$

APPENDIX B

DCS and Marginal Cases from Data Set Used for Fitting

- Outcome = **D** for DCS
  = **M** for Marginal
- Dupes = Number of divers showing same outcome
- Bottom Depth in feet of sea water
- Bottom Time in minutes
- Surface Time = Surfacing time in minutes, *i.e.* length of dive
- T1 = Last time definitely free of symptoms
- T2 = Time of reported symptoms

- Rules for determining T1: (from 5,6)

Reported T2	T1 by Rules
Tsurf + 180 min or more	Tsurf + 120 min
Tsurf + 60 to 180 min	Tsurf + 30 min
Tsurf + 20 to 60 min	Tsurf + 10 min
Tsurf + less than 20 min	Time leaving last stop depth
Before Tsurf	Time leaving second previous stop depth

- Some T1s obtained from dive records, not from rules.

- Some Marginal cases do not have time of symptoms information.

COMMENT	PROFILE	OUTCOME	DUPES	BOTTOM DEPTH	BOTTOM TIME	SURFACE TIME	T1	T2
			EDU885A					
AN1003.OUT REPETS= 1	3	D	1	150.0	52.5	320.1	319.9	325.1
AN1003.OUT REPETS= 1	4	D	1	150.0	52.5	320.1	350.1	440.1
AN1005.OUT REPETS= 1	7	D	1	60.0	177.0	336.4	456.0	756.0
AN1010.OUT REPETS= 1	13	D	1	150.0	55.3	215.3	165.5	275.0
AN1010.OUT REPETS= 2	14	D	1	150.0	55.3	354.5	475.0	775.0
AN1010.OUT REPETS= 2	15	D	1	150.0	55.3	354.5	475.0	1495.0
AN1012.OUT REPETS= 1	18	D	1	60.0	178.2	254.1	374.0	554.0
AN1012.OUT REPETS= 1	19	D	1	60.0	178.2	254.1	374.0	524.0
AN1012.OUT REPETS= 1	20	D	1	60.0	178.2	254.1	182.2	494.0
AN1013.OUT REPETS= 1	22	D	1	60.0	178.7	293.8	203.6	293.6
AN1013.OUT REPETS= 1	23	D	1	60.0	178.7	293.8	323.8	444.0
AN1013.OUT REPETS= 1	24	D	2	60.0	178.7	293.8	323.8	474.0
AN1015.OUT REPETS= 1	27	D	1	120.0	54.7	154.3	64.0	154.1
AN1021.OUT REPETS= 1	34	D	1	147.0	35.3	134.2	254.0	434.0
AN1024.OUT REPETS= 2	38	D	1	150.0	35.7	139.2	259.0	559.0
AN1032.OUT REPETS= 1	47	D	1	190.0	35.6	281.5	311.5	461.0
AN1032.OUT REPETS= 1	48	D	1	190.0	35.6	281.5	401.0	521.0
AN1039.OUT REPETS= 1	56	D	1	120.0	76.6	350.0	470.0	770.0
AN1039.OUT REPETS= 1	57	D	1	120.0	76.6	350.0	470.0	2680.0
AN1041.OUT REPETS= 1	60	D	1	120.0	67.1	285.6	72.9	287.6
AN1041.OUT REPETS= 1	61	D	1	120.0	67.1	285.6	406.0	1246.0
AN1045.OUT REPETS= 1	64	D	1	120.0	57.0	212.0	242.0	362.0
AN2002.OUT REPETS= 1	67	D	1	150.0	36.5	146.7	88.0	146.7
AN2012.OUT REPETS= 1	73	D	1	100.0	57.0	135.7	65.9	155.7
AN2017.OUT REPETS= 1	75	D	1	100.0	27.6	37.4	47.4	77.4
AN2019.OUT REPETS= 1	77	D	1	100.0	27.1	37.2	33.2	42.2
AN2019.OUT REPETS= 1	78	D	1	100.0	27.1	37.2	33.2	62.2
AN2019.OUT REPETS= 1	79	D	1	100.0	27.1	37.2	33.2	77.2
AN2020.OUT REPETS= 1	80	D	1	80.0	117.3	339.1	459.0	1299.0
			DC4W					
DR0003A REPETS= 1	1	D	1	117.0	47.3	107.7	228.0	1188.0
DR0016A REPETS= 1	11	D	1	148.0	27.1	77.2	197.2	857.0
DD1695A REPETS= 1	31	D	1	199.0	20.0	107.1	135.0	165.0
DD1695A REPETS= 1	32	M	1	199.0	20.0	107.1	135.0	255.0
DR0209A REPETS= 1	70	M	1	148.0	27.5	87.7	30.0	208.0
DD1916A REPETS= 1	109	M	1	57.0	59.1	70.1	157.0	307.0
DD1918A REPETS= 1	112	M	1	65.0	58.9	70.2	187.1	427.0
DD1933A REPETS= 1	124	D	1	198.0	5.8	21.4	138.3	288.0
DD1936A REPETS= 1	127	D	1	231.0	2.8	19.8	12.8	29.8

DD1936A REPETS= 1	128	D	1	231.0	2.8	19.8	136.7	737.0
DD2000A REPETS= 1	131	D	1	168.0	6.1	37.1	64.0	94.0
DD1693A REPETS= 1	141	D	1	149.0	38.0	128.1	244.0	364.0
EDU885AR								
AN2010.OUT REPETS= 2	2	D	1	100.0	105.7	301.4	301.1	334.1
AN2010.OUT REPETS= 3	3	D	1	100.0	105.7	471.9	205.0	481.9
AN2010.OUT REPETS= 3	4	D	1	100.0	105.7	471.9	592.0	892.0
AN2011.OUT REPETS= 2	6	D	1	150.0	61.2	459.2	458.9	464.2
AN2011.OUT REPETS= 2	7	D	1	150.0	61.2	459.2	579.2	1719.0
AN2017.OUT REPETS= 2	10	D	1	100.0	43.9	123.8	243.8	334.0
AN3001.OUT REPETS= 2	15	D	1	80.0	76.3	282.9	280.7	292.9
AN3003.OUT REPETS= 2	18	D	1	80.0	67.0	175.4	173.3	188.4
AN3004.OUT REPETS= 3	20	D	1	100.0	53.8	198.1	195.4	318.0
AN3004.OUT REPETS= 3	21	D	1	100.0	53.8	198.1	318.0	438.0
AN3007.OUT REPETS= 2	25	D	1	78.0	66.6	175.8	206.0	266.0
DC4WR								
DR0278A REPETS=2	3	D	1	147.6	40.0	282.2	229.1	292.2
DR0272R REPETS=2	6	D	1	118.1	54.6	268.2	388.0	868.0
DR0285R REPETS=2	9	D	1	177.2	26.6	330.6	329.5	345.6
SUBX87								
20xbx2v.dat	49	D	1	506.4	0.1	1.5	0.5	4.5
22xax1u.dat	57	D	1	580.2	0.1	2.0	0.8	12.0
NMRNSW								
NSW1C03	4	M	1	61.5	79.0	85.9	206.0	266.0
NSW1C06	8	D	1	61.5	90.0	97.5	127.5	217.5
NSW1C12	15	M	1	61.5	90.8	106.7	227.0	297.0
NSW1C13	17	M	1	61.5	100.1	107.9	117.9	137.9
NSW1C14	19	D	1	61.5	99.0	111.5	141.5	204.5
nsw1c16	22	M	1	61.5	100.1	106.7		
nsw1c16	23	D	1	61.5	100.1	106.7	226.7	467.0
NSW1C17	25	D	1	61.5	90.2	97.7	217.7	608.0
NSW1C19	28	D	1	61.5	79.7	86.1	96.1	121.1
NSW1E07	36	M	1	61.5	300.2	308.3		
NMR8697								
DRA4:[WEATHERSBY.DLE]8301	6	D	1	71.0	28.9	31.5	151.5	271.5
DRA4:[WEATHERSBY.DLE]8301	7	M	1	71.0	28.9	31.5	91.5	151.5
DRA4:[WEATHERSBY.DLE]8301	9	M	1	71.0	28.7	31.5	151.5	391.5
DRA4:[WEATHERSBY.DLE]8301	15	M	1	75.0	28.6	31.6	36.6	91.6
DRA4:[WEATHERSBY.DLE]8301	44	M	1	105.0	28.2	32.1	92.1	152.1
DRA4:[WEATHERSBY.DLE]8301	58	D	1	125.0	28.1	32.4	152.4	272.4
DRA4:[WEATHERSBY.DLE]8301	65	D	1	130.0	27.6	32.5	32.5	36.5

DRA4:[WEATHERSBY.DLE]8301	74	D	1	46.0	59.3	61.1	121.1	166.1
DRA4:[WEATHERSBY.DLE]8301	76	D	1	46.0	59.2	61.1	181.1	781.1
DRA4:[WEATHERSBY.DLE]8301	94	M	1	56.0	58.4	61.3	181.3	421.3
DRA4:[WEATHERSBY.DLE]8[illegible]	98	M	1	59.0	59.0	61.3	121.3	181.3
DRA4:[WEATHERSBY.DLE]8301	105	M	1	72.0	58.7	61.5	181.5	301.5
DRA4:[WEATHERSBY.DLE]8301	116	M	1	80.0	58.7	61.7	181.7	421.7
DRA4:[WEATHERSBY.DLE]8301	119	M	1	80.0	58.6	61.7	66.7	81.7
DRA4:[WEATHERSBY.DLE]8301	126	M	1	88.0	59.3	61.8	66.8	81.8
DRA4:[WEATHERSBY.DLE]8301	132	D	1	88.0	58.5	61.8	181.8	241.8
DRA4:[WEATHERSBY.DLE]8301	143	D	1	96.0	58.3	61.9	66.9	81.9
DRA4:[WEATHERSBY.DLE]8301	162	D	1	29.0	239.1	240.8	360.8	660.8
DRA4:[WEATHERSBY.DLE]8301	173	D	1	33.0	239.3	240.9	360.9	600.9
DRA4:[WEATHERSBY.DLE]8301	176	M	1	34.0	239.6	240.9	300.9	360.9
DRA4:[WEATHERSBY.DLE]8301	180	M	1	34.0	238.7	240.9	300.9	360.9
DRA4:[WEATHERSBY.DLE]8301	181	M	1	35.0	239.5	240.9	245.9	300.9
DRA4:[WEATHERSBY.DLE]8301	184	D	1	35.0	238.6	240.9	245.9	300.9
DRA4:[WEATHERSBY.DLE]8301	186	M	1	36.0	239.5	240.9	300.9	390.9
DRA4:[WEATHERSBY.DLE]8301	193	D	1	50.0	239.1	241.2	361.2	601.2
DRA4:[WEATHERSBY.DLE]8301	208	M	1	58.0	238.6	241.3	301.3	361.3
DRA4:[WEATHERSBY.DLE]8301	221	M	1	70.0	237.1	241.5	301.5	361.5
DRA4:[WEATHERSBY.DLE]8301	223	M	1	74.0	238.8	241.6	361.6	451.6
DRA4:[WEATHERSBY.DLE]8301	226	M	1	74.0	238.3	241.6	361.6	601.6
EDU885M								
AN2003.O REPETS= 1	6	D	1	150.0	56.7	286.5	407.0	467.0
AN2003.O REPETS= 1	7	D	1	150.0	56.7	286.5	317.0	437.0
AN2007.O REPETS= 1	10	D	1	150.0	36.3	130.8	251.0	971.0
AN2007.O REPETS= 1	11	D	1	150.0	36.3	130.8	251.0	1211.0
EDU885S								
*** [.EDURAW]AN3010.OUT;1	6	D	1	100.0	20.1	328.8	449.0	569.0
*** [.EDURAW]AN3012.OUT;1	8	D	1	80.0	107.8	369.7	490.0	1210.0
*** [.EDURAW]AN3012.OUT;1	9	D	1	80.0	107.8	369.7	490.0	4690.0
*** [.EDURAW]AN3014.OUT;1	11	D	1	100.0	20.0	344.4	374.4	464.4
EDU184								
MDC018.OUT REPETS= 3	1	D	1	60.0	158.5	353.5	348.9	363.5
MDC021.OUT REPETS= 3	5	D	1	100.0	49.0	248.0	243.0	258.0
MDC024.OUT REPETS= 4	11	D	1	80.0	101.9	364.7	360.9	365.7
MDC024.OUT REPETS= 4	12	D	1	80.0	101.9	364.7	277.2	374.7
MDC027.OUT REPETS= 3	16	D	1	150.0	49.0	385.2	384.2	390.2
MDC027.OUT REPETS= 2	17	D	1	150.0	49.0	300.0	299.1	315.0
MDC028.OUT REPETS= 1	21	D	1	150.0	23.8	92.9	71.6	92.9
MDC028.OUT REPETS= 3	22	D	1	150.0	47.7	312.1	322.1	352.1
MDC028.OUT REPETS= 4	23	D	1	150.0	47.7	397.0	312.1	407.0
MDC034.OUT REPETS= 3	33	D	1	60.0	145.7	323.3	333.3	348.3
MDC035.OUT REPETS= 2	35	D	1	150.0	61.0	351.3	331.7	355.4

EDU1180S

DIV361 REPETS= 1	1	D	1	150.0	61.1	222.0	252.0	312.0
DIV361 REPETS= 1	2	D	1	150.0	61.1	222.0	252.0	327.0
DIV461 REPETS= 1	4	D	1	149.0	57.7	261.0	381.0	681.0
DIV562 REPETS= 1	7	D	1	150.0	60.4	220.0	230.0	265.0
DIV562 REPETS= 1	8	D	1	150.0	60.4	220.0	340.0	700.0
DIV562 REPETS= 1	9	D	1	150.0	60.4	220.0	91.4	240.0
DIV571 REPETS= 1	11	D	1	150.0	45.4	173.0	203.0	233.0
DIV571 REPETS= 1	12	D	1	150.0	45.4	173.0	293.0	593.0
DIV571 REPETS= 1	13	D	1	150.0	45.4	173.0	203.0	263.0
DIV581 REPETS= 1	15	D	1	100.0	59.6	127.0	157.0	217.0

ASATEDU

NEDU TEST79-8 REPETS= 1	2	D	1	60.0	2756.0	4020.0	3225.0	3945.0
NEDU TEST79-8 REPETS= 1	3	D	1	60.0	2756.0	4020.0	3270.0	3990.0
NEDU TEST79-8 REPETS= 1	4	D	1	60.0	2756.0	4020.0	3120.0	3840.0
NEDU TEST79-8 REPETS= 1	5	D	1	60.0	2756.0	4020.0	4140.0	6900.0
NEDU TEST79-30 REPETS= 1	7	D	1	60.0	4891.0	6516.0	5946.0	6666.0
NEDU TEST79-30 REPETS= 1	8	D	1	60.0	4891.0	6516.0	6006.0	6726.0
NEDU TEST79-30 REPETS= 1	9	D	1	60.0	4891.0	6516.0	5916.0	6636.0
NEDU TEST79-38 REPETS= 1	11	D	1	60.0	5643.0	7300.0	6730.0	7450.0
NEDU TEST79-38 REPETS= 1	12	M	3	60.0	5643.0	7300.0		
NEDU TEST81-8 RECOMP 12-2	14	D	1	60.0	5814.5	7881.0	5820.0	6560.0
NEDU TEST81-13, REPETS=	16	M	4	60.0	5888.0	7518.0		
NEDU TEST81-13, REPETS=	17	D	1	60.0	5888.0	7518.0	6797.0	7517.0
NEDU TEST82-41 REPETS= 1	18	M	10	60.0	5566.0	7332.0		
NEDU TEST83-42 EXCURS= 1	19	D	1	60.0	5524.0	7343.0	7463.0	7823.0
NEDU TEST83-42 EXCURS= 1	20	M	7	60.0	5524.0	7343.0		
NEDU TEST83-42 REPET = 1	21	M	2	60.0	5578.0	7343.0		
NEDU TEST84-42 REPETS= 1	25	M	1	60.0	5637.0	7484.0	5643.0	6095.0
NEDU TEST86-06 EXCURS= 9	28	D	1	60.0	4066.0	6536.0	6656.0	7231.0
NEDU TEST88-03 EXCURS= 1	32	D	1	50.0	3588.0	7204.0	4320.0	7494.0

ASATNSM

MINISAT-1 (fatigue)	2	M	13	25.5	2878.0	2881.3		
MINISAT-1 (niggles)	3	M	1	25.5	2878.0	2881.3	3001.0	3601.0
MINISAT-1 (niggles)	4	M	1	25.5	2878.0	2881.3	2891.0	2911.0
MINISAT-1 (niggles)	5	M	2	25.5	2878.0	2881.3	3001.0	3180.0
MINISAT-2	7	D	1	29.5	2878.0	2881.4	2911.0	2946.0
MINISAT-2	8	D	1	29.5	2878.0	2881.4	2911.0	2961.0
MINISAT-2	9	D	1	29.5	2878.0	2881.4	2911.0	2971.0
MINISAT-2	10	D	1	29.5	2878.0	2881.4	2911.0	3031.0
MINISAT-2 (niggles)	11	M	1	29.5	2878.0	2881.4	2911.0	3031.0
MINISAT-2 (niggles)	12	M	1	29.5	2878.0	2881.4	3001.0	3241.0
MINISAT-2 (fatigue)	13	M	1	29.5	2878.0	2881.4		
AIRSAT-1+LAST EXCURS	15	D	1	60.0	9828.0	11520.0	10579.0	11299.0
AIRSAT-2 +LAST EXCURS	17	M	1	60.0	11475.5	12960.0	12420.0	13140.0
AIRSAT-3B+last excurs	19	D	1	132.0	6887.2	10297.7	9455.0	10175.0

AIRSAT-3D +last 198 excur	22	D	1	132.0	6617.6	10038.0	9213.0	9933.0
AIRSAT-3D +last 198 excur	23	D	1	132.0	6617.6	10038.0	9758.0	10478.0
AIRSAT4-D,	26	D	1	132.0	3580.0	7508.0	6609.0	7329.0
AIRSAT-5F	31	D	1	111.0	2867.5	6590.0	2880.0	3175.0
AIRSAT-5D	33	D	1	111.0	2867.5	8700.0	4631.0	5351.0
AIRSAT-5E(TRUNC)	34	D	3	111.0	2867.5	2882.9	2880.0	3210.0
AIRSAT-5G(TRUNC)	36	D	2	111.0	2865.5	2882.0	2880.0	3009.0
AIRSAT-5G(TRUNC SH)	37	D	1	111.0	2865.5	6528.0	5808.0	6528.0
AIRSAT-5I	40	D	1	111.0	2870.9	8306.8	5252.0	5972.0
	ASATNMR							
NMRI JUL88	34	D	1	24.0	4319.6	4320.4	4440.0	4485.0

TABLE 1

Summary of Data Set Used in Modelling.

	Profiles	Man-dives	% of Total Dives	DCS	Marg*	w/TOB**	%DCS
Single Air							
EDU885A	82	483	20.3%	30	-	30	6.2%
DC4W	143	244	10.2	8	4	12	3.4
SUBX87	58	58	2.4	2	-	2	3.4
NMRNSW	45	91	3.8	5	5	8	6.0
Total ____	328	876	36.8	45	9	52	5.2
Repetitive Air							
EDU885AR	31	182	7.6%	11	-	11	6.0%
DC4WR	9	12	0.5	3	-	3	25.0
Total ____	40	194	8.1	14	-	14	7.2
Single non-Air							
NMR8697	229	477	20.0%	11	18	29	2.7%
EDU885M	13	81	3.4	4	-	4	4.9
EDU885S	14	94	3.9	4	-	4	4.3
EDU1180S	22	120	5.0	10	-	10	8.3
Total ____	278	772	32.4	29	18	47	4.0
Repetitive non-Air							
EDU184	42	239	10.0%	11	-	11	4.6%
Total ____	42	239	10.0	11	-	11	4.6
Saturation							
ASATEDU	32	120	5.0%	13	27	14	13.1%
ASATNSM	45	132	5.5	18	21	25	15.2
ASATNMR	34	50	2.1	1	-	1	2.0
Total ____	111	302	12.7	32	48	40	12.2
Grand Total	799	2383	100.0%	131	75	164	5.8%

* Marginal DCS = 0.1 DCS case
** TOB = Time of DCS Occurrence

TABLE 2

Log Likelihood Results for Linear/Exponential Models.

	MODEL	Type	Log Likelihood	# of Estimated Parameters
	(constant risk; r = .00003)	Null	-888.28	1
1a. -	3 tiss. exponential, no THR	EE1	-708.77	6
1b. -	3 tiss. exponential, w/ THR	EE1	-707.58	9
1c. -	4 tiss. exponential, no THR	EE1	-708.55	8
1d. -	4 tiss. exponential, w/ THR	EE1	-706.67	10
1e. -	3 tiss. linear-exp., no THR	LE1	-700.11	7
1f. -	**3 tiss. linear-exp., w/ THR**	**LE1**	**-696.54**	**8**
1g. -	4 tiss. linear-exp., no THR	LE1	-698.16	9
1h. -	**4 tiss. linear-exp., w/ THR**	**LE1**	**-687.77**	**11**
2a. -	3 tiss. exponential, no THR	EE2	-775.32	6
2b. -	**3 tiss. exponential, w/ THR**	**EE2**	**-744.23**	**9**
2c. -	3 tiss. linear-exp., no THR	LE2	-774.71	9
2d. -	3 tiss. linear-exp., w/ THR	LE2	-743.53	12

TABLE 3

Parameter Estimates and (Standard Errors).

	MODELS		
PARAMETER	1f.	1h.	2b.
α_A (min)	1.47 (0.70)	1.49 (0.70)	2.49 (0.91)
α_B	50.80 (19.11)	52.25 (19.29)	84.63 (6.86)
α_C	487.60 (41.39)	489.91 (47.29)	526.21 (59.94)
α_D		1188.60 (4.5E+5)	
G_A	4.3E-3 (3.3E-3)	4.3E-3 (3.3E-3)	3.8E-4 (1.7E-4)
G_B	1.1E-4 (4.0E-5)	1.1E-4 (4.0E-5)	5.4E-6 (9.4E-7)
G_C	1.0E-3 (1.9E-4)	8.7E-4 (1.9E-4)	7.5E-7 (1.8E-7)
G_D		1.15 (690.)	
PXO_A (fsw)	∞	∞	∞
PXO_B	1.06 (0.84)	1.06 (0.77)	∞
PXO_C	∞	∞	∞
PXO_D		∞	
THR_A (fsw)	0.0	0.0 (4.92)	3.76
THR_B	0.0	0.0 (0.44)	2.57
THR_C	1.75 (0.68)	1.54 (0.80)	3.24 (1.10)
THR_D		30.56 (8493.)	

TABLE 4

Comparison of Total Number of DCS Cases Observed and Predicted for Component Data Sets.

	Man-Dives	OBS DCS	PREDICTED DCS: 1f.	1h.	2b.
Single Air					
EDU885A	483	30.0	27.7	27.3	29.6
DC4W	244	8.4	6.0	6.1	8.5
SUBX87	58	2.0	0.7	0.7	0.8
NMRNSW	91	5.5	5.4	5.2	6.3
Total	876	45.9	39.8	39.3	45.2
Repetitive Air					
EDU885AR	182	11.0	12.2	12.4	13.9
DC4WR	12	3.0	1.0	1.0	1.1
Total	194	14.0	13.2	13.4	15.0
Single non-Air					
NMR8697	477	12.8	15.9	15.7	20.3
EDU885M	81	4.0	3.6	3.6	4.1
EDU885S	94	4.0	4.2	4.2	3.9
EDU1180S	120	10.0	7.5	7.3	7.5
Total	772	30.8	31.2	30.8	35.8
Repetitive non-Air					
EDU184	239	11.0	14.6	14.5	12.3
Total	239	11.0	14.6	14.5	12.3
Air Saturation					
ASATEDU	120	15.7	14.4	13.3	9.5
ASATNSM	132	20.1	21.2	23.9	20.5
ASATNMR	50	1.0	4.5	4.1	2.5
Total	302	36.8	40.1	41.3	32.5
Grand Total	2383	138.5	138.9	139.3	140.7

TABLE 5

Model Prediction of Total Number of DCS Case Occurrence Stratified by Estimated Risk Level

	MODELS											
	NULL			**1f.**			**1h.**			**2b.**		
RISK CATEGORY	# DIVES	DCS OBS	DCS PRED	# DIVES	DCS OBS	DCS PRED	# DIVES	DCS OBS	DCS PRED	# DIVES	DCS OBS	DCS PRED
0.0 - 2.5%	63	2.0	1.3	535	13.9	9.8	521	13.8	9.7	209	6.1	3.6
2.5 - 5.0%	1771	77.7	78.3	614	21.9	22.9	646	22.0	24.3	916	29.5	34.9
5.0 - 7.5%	257	25.0	13.4	643	27.6	39.6	659	30.7	40.5	777	38.3	48.9
7.5 - 10.0%	57	12.0	4.7	298	31.7	25.4	325	35.0	28.0	312	37.1	26.3
10.0 - 100.%	235	21.8	42.1	293	43.4	41.4	232	37.0	36.8	169	27.5	26.9
χ^2 = (df = 4)			31.1			7.1			6.1			9.3

TABLE 6

Observed and Predicted DCS Onset Times.

		Predicted DCS			
Time Category	OBS DCS	NULL	1f.	1h.	2b.
Before Surfacing	26.5	56.0	30.4	29.4	18.5
Surfacing to +30 min	12.2	1.7	15.2	17.1	12.3
+30 min to +2 hr	26.0	5.2	27.6	26.6	22.5
+2 hr to +4 hr	23.3	6.9	21.8	21.0	28.1
+4 hr to +24 hr	20.8	67.7	12.0	12.2	28.2
		χ^2 = 215.5 (df = 4)	4.3	4.5	3.4

TABLE 7

Observed and Predicted DCS for Data not used in Modelling (95% confidence limits).

	Man-Dives	OBS DCS	PREDICTED DCS 1f.	PREDICTED DCS 1h.	PREDICTED DCS 2b.
Single Air					
DC4D	797	19.4	**16.8** (11.8-21.8)	**17.1** (11.8-22.4)	**23.9** (17.7-30.2)
Repetitive Air					
DC4DR	142	1.0	**7.0** (5.4-8.7)	**7.1** (5.4-8.8)	**8.0** (6.2-9.7)
Repetitive non-Air					
EDU1180R	128	2.0	**13.4** (10.6-16.1)	**12.6** (9.9-15.3)	**10.1** (6.5-13.1)
Air & O_2 Decompression					
DC8AOW	46	3.1	**0.4** (0.2-0.6)	**0.4** (0.2-0.6)	**0.6** (0.4-0.7)
DC8AOD	256	3.2	**1.9** (0.8-2.9)	**2.0** (0.8-3.2)	**2.1** (1.4-2.7)
Surface Decompression					
DC8ASUR	358	10.1	**3.5** (1.4-5.6)	**3.6** (1.3-5.9)	**2.1** (1.4-2.9)
DCSUREP	69	1.0	**1.0** (0.5-1.5)	**1.1** (0.5-1.6)	**0.8** (0.5-1.1)
SUREX	24	5.3	**4.1** (3.0-5.2)	**23.9** (-170.-218.)	**2.5** (1.7-3.3)
Non-Air Saturation					
ASATARE	165	21.3	**18.3** (13.3-23.3)	**16.6** (-1515.-1548.)	**10.0** (6.5-13.6)

FIGURE LEGENDS

Figure 1. Linear-Exponential Tissue Pressures and Risk Functions.

Tissue pressures are plotted using a 50 minute time constant, with PXOs of 1000 and 15 fsw. The two instantaneous risks functions are plotted for both of The above tissue pressure curves.

Figure 2. Distribution of Time of Symptoms (T2).

Number of DCS cases reported is plotted versus time of reported occurrence after dive surfacing.

Figure 3. Effect of Including Metabolic Gases.

Tissue pressures are plotted for the current EE1 model and for a previous model which was unable to reach the T1 time for this dive. The same exponential time constant is used for both models. The increase in tissue pressure due to including metabolic gases allows EE1 to have a positive instantaneous risk beyond time T1.

Figure 4. Observed and Predicted DCS for the Fitted Data.

The number of DCS cases observed in each type-of-dive group is shown with the prediction and 95% confidence limits for the three selected models (1f,1h,2b).

Figure A1. LE1/EE1 Risk Calculations.

FIGURE 1

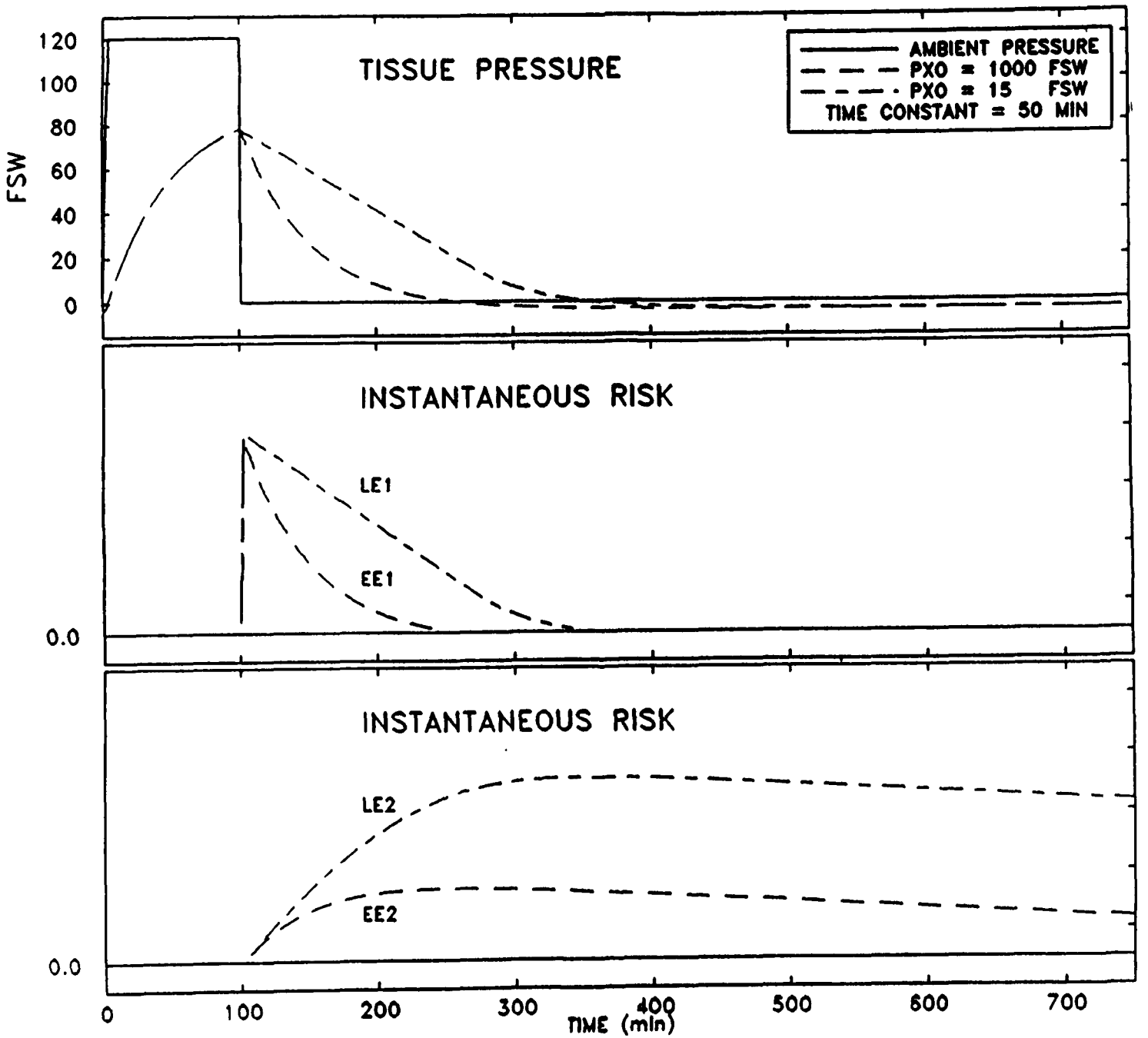
TISSUE PRESSURE
AMBIENT PRESSURE
PXO = 1000 FSW
PXO = 15 FSW
TIME CONSTANT = 50 MIN
FSW
120
100
80
60
40
20
0
INSTANTANEOUS RISK
LE1
EE1
0.0
INSTANTANEOUS RISK
LE2
EE2
0.0
0
100
200
300
400
500
600
700
TIME (min)

FIGURE 2

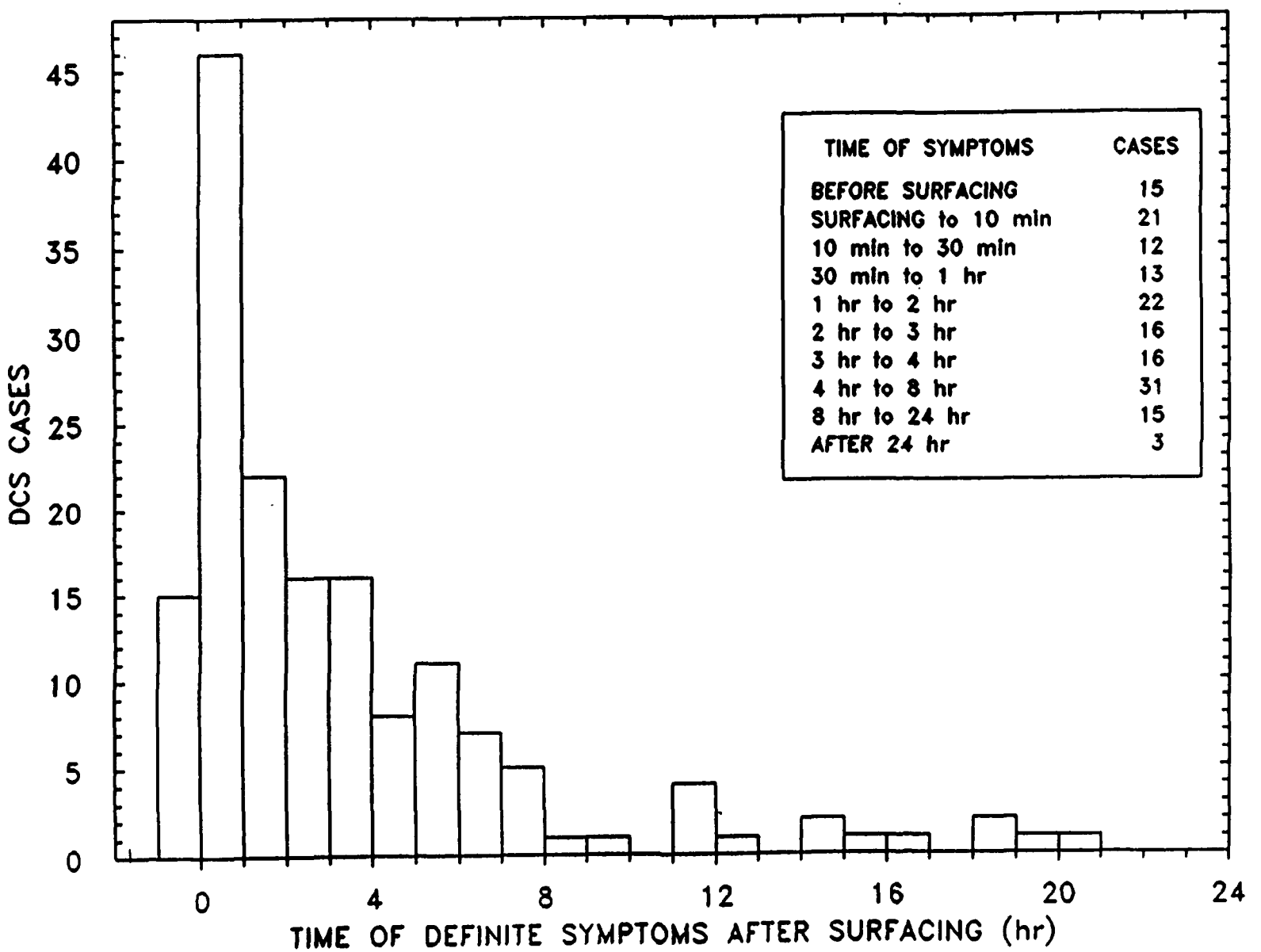
DCS CASES
45
40
35
30
25
20
15
10
5
0
0
4
8
12
16
20
24
TIME OF DEFINITE SYMPTOMS AFTER SURFACING (hr)
TIME OF SYMPTOMS CASES
BEFORE SURFACING 15
SURFACING to 10 min 21
10 min to 30 min 12
30 min to 1 hr 13
1 hr to 2 hr 22
2 hr to 3 hr 16
3 hr to 4 hr 16
4 hr to 8 hr 31
8 hr to 24 hr 15
AFTER 24 hr 3

FIGURE 3

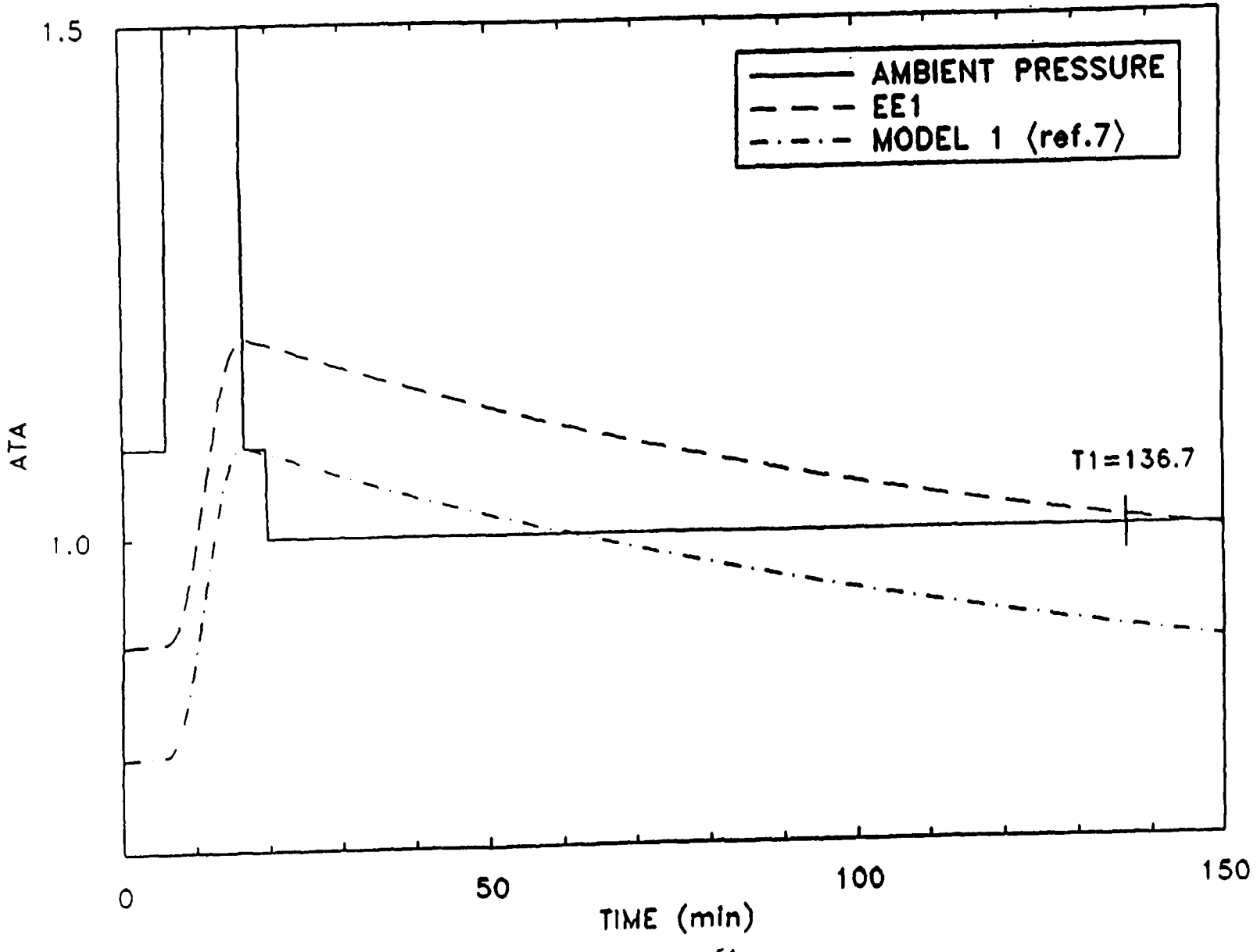
1.5
1.0
ATA
AMBIENT PRESSURE
EE1
MODEL 1 ⟨ref.7⟩
T1=136.7
0
50
100
150
TIME (min)

FIGURE 4

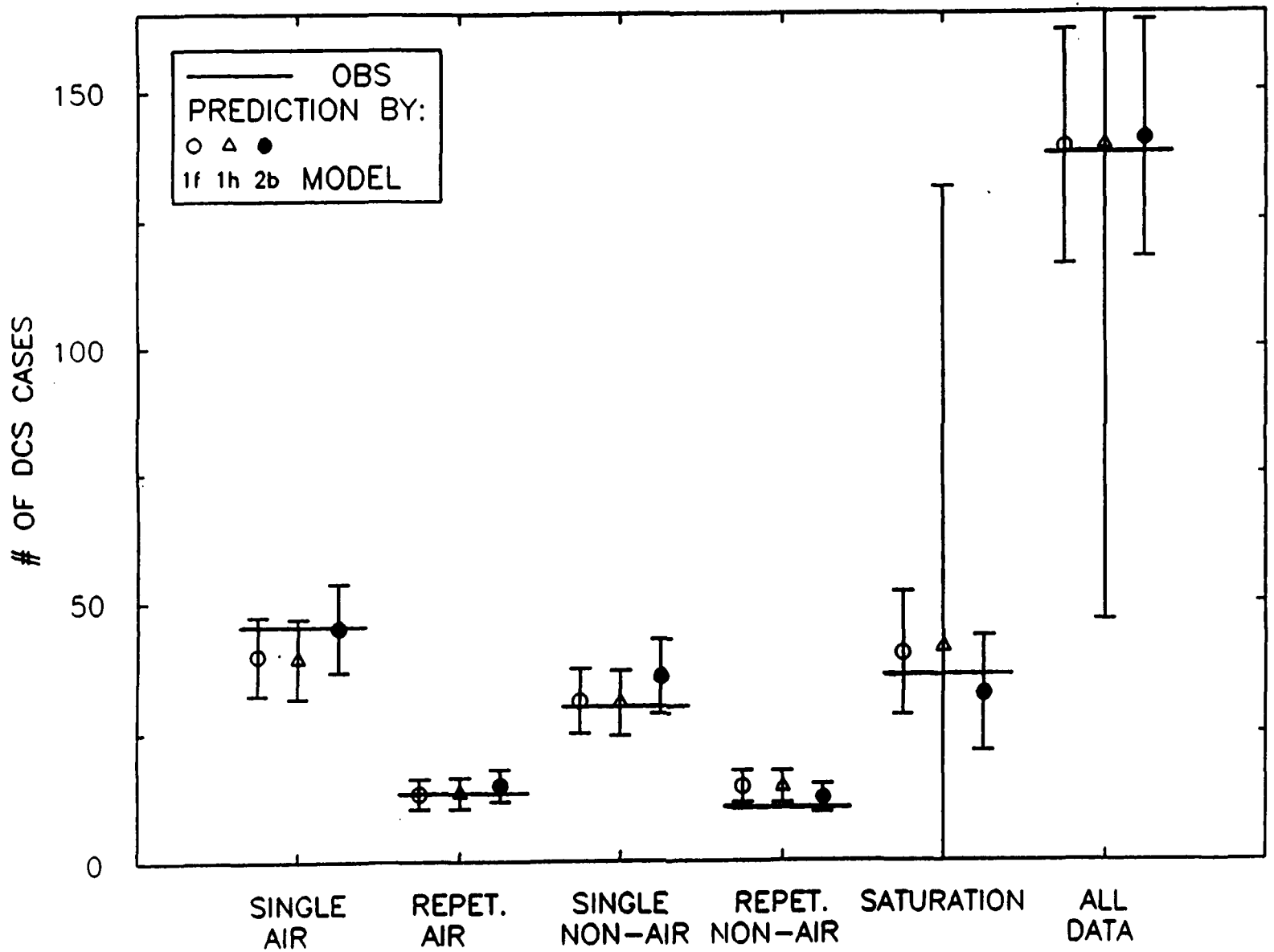
OBS
PREDICTION BY:
1f 1h 2b MODEL
OF DCS CASES
150
100
50
0
SINGLE AIR
REPET. AIR
SINGLE NON-AIR
REPET. NON-AIR
SATURATION
ALL DATA